



Low Reynolds number flows across ordered arrays of micro-cylinders embedded in a rectangular micro/minichannel

A. Tamayol^{a,*}, J. Yeom^{b,1}, M. Akbari^a, M. Bahrami^a

^a Laboratory for Applied Energy Conversion (LAEC), School of Engineering Science, Simon Fraser University, Surrey, BC, Canada V3T 0A3

^b Department of Mechanical Science and Engineering, University of Illinois at Urbana-Champaign, Urbana, IL 61801, USA

ARTICLE INFO

Article history:

Received 22 February 2012

Received in revised form 28 October 2012

Accepted 29 October 2012

Keywords:

Porous media filled channels

Pressure drop

Brinkman equation

Variable cross-section channels

Creeping flow

ABSTRACT

Pressure drop of ordered arrays of cylinders embedded inside microchannels is experimentally and analytically studied. Two independent modeling techniques are used to predict the flow resistance for the creeping flow regime. The pressure drop is expressed as a function of the involved geometrical parameters such as micro-cylinder diameter, spacing between adjacent cylinders, channel height, and its width. To verify the developed models, 15 silicon/glass samples are fabricated using the deep reacting ion etching (DRIE) technique. Pressure drop measurements are performed over a wide range of nitrogen flow rates spanning from 0.1 sccm to 35 sccm. Both methods predict the trend of the experimental data. The porous medium approach shows a wider range of applicability with reasonable accuracy while the variable cross-section technique is more accurate for dense arrays of micro-cylinders. Our results suggest that an optimal micro-cylinder diameter exists that minimizes the pressure drop for a specific surface-area-to-volume ratio. This diameter is a function of the channel dimensions and the desired surface-area-to-volume ratio.

© 2012 Elsevier Ltd. All rights reserved.

1. Introduction

Flow across arrays of micro-cylinders embedded inside mini/microchannels is of great importance for various applications such as microreactors [1,2], micro heat exchangers [3–5], micro-total analysis systems (μ TAS) [6], and microfilters [7]. These micro-cylinders enhance heat and mass transfer coefficients, surface-area-to-volume ratio, surface chemical reactions, and thermal conductance with the penalty of a reduction in the effective cross-sectional area. The reduced flow area results in an overall pressure drop increase. As a result of this competitive trend, an optimum design(s) can be found for various applications. This, however; requires an accurate model that can predict the pressure drop as a function of the salient geometrical parameters of the micro-cylinder-embedded-microchannel assembly.

The creeping flow across ordered arrays of cylinders has been the subject of numerous studies; see for example references [8–12]. Many of these studies provided analytical expressions for the flow resistance (the ratio of pressure drop over volumetric flow rate) of two-dimensional flow across a periodic array of circular cylinders, which is usually applicable to high aspect ratio systems. However, employing the existing models may lead to significant inaccuracy

in the analysis of flow through low aspect ratio cylinders embedded inside channels. The experimental results reported by Kosar et al. [3], Vanapalli et al. [13], and Yeom et al. [14] revealed that in the case of low aspect ratio cylinders, these two-dimensional models failed. Therefore, a more general model should consider the channel walls' effects in the analysis in order to successfully predict the flow through the cylinder array.

In this study, we adopt and compare two different approaches for modeling the flow across arrays of micro-cylinders embedded inside microchannels of low aspect ratio:

- (i) The porous medium approach in which the problem is modeled as a channel filled with a porous medium.
- (ii) The variable cross-section channel approach, where the flow between cylinders is modeled as the flow along a variable cross-section microchannel.

Fully developed and developing flows in channels of various cross-sections filled with porous media have been extensively studied in the literature (see for example [15–19]); however, such studies for small-scale mini- and micro-size channels are not numerous. Gamarat et al. [20] employed volume averaged equations to study flow through channels partially filled with micro-posts in an attempt to investigate effects of wall roughness on the flow field and pressure drop. They also performed experimental investigations and successfully compared their theoretical analysis

* Corresponding author.

E-mail address: ali_tamayol@sfu.ca (A. Tamayol).

¹ These authors have contributed equally to this work.

Nomenclature

d	cylinder diameter, m
$E(\cdot)$	uncertainty associated with measured parameters
f	Fanning friction factor
h	channel depth, m
H^*	dimensionless parameter used in Eq. (10), $H^* = h/d$
I_p	cross-sectional polar moment of inertia, m^4
I_p^*	dimensionless cross-sectional polar moment of inertia, $I_p^* = I_p/A^2$
K	permeability, m^2
L	channel length, m
P	pressure, N/m^2
Q	volumetric flow rate (sccm)
Re	Reynolds number
S	distance between centers of adjacent cylinders, m
U	volume averaged velocity, m/s

Greek symbols

ϕ'	parameter used in Eq. (5)
ε	porosity
ε'	local cross-sectional aspect ratio
μ	viscosity, $N\ s/m^2$
μ_{eff}	effective viscosity, $N\ s/m^2$
μ'	viscosity ratio, $\mu' = \mu_{eff}/\mu$

Subscript

c	related to connections
D	developing
FD	fully developed
minor	minor losses
ev	electro viscous

with the experimental data. Recently, Tamayol et al. [21] used volume averaged equations for predicting the pressure drop inside microchannels filled with ordered arrays of cylinders. To verify their analysis, they fabricated five samples using the soft lithography technique [22,23] and measured the pressure drop of the samples over a range of volumetric flow rates. Moreover, they employed a numerical approach for determining the flow through the fabricated samples' geometry. The numerical and experimental data were in a reasonable agreement with their model.

In the variable cross-section approach, it is postulated that the passing fluid experiences a channel-like flow between cylinders with a variable cross-sectional area; the flow resistance can be obtained by either lubrication approximation [24] or asymptotic series solution [25,26]. The latter approach provides a more accurate estimation for pressure drop when the inertial effect becomes significant and/or the variation in the cross-sectional area becomes substantial [25]. In this approach, the solution of the Navier–Stokes equations is obtained by expanding the flow variables in powers of a small parameter characterizing the slowly varying geometry of the bounding walls, usually referred as a perturbation parameter [25]. In the lubrication approach, the flow is assumed to be fully developed at each cross-section. The overall pressure drop is then calculated by integrating the local pressure gradient over the total length of the channel. Although the asymptotic solution method gives more accurate results than the lubrication approximation, the final solution for the pressure drop and velocity field has a complex form.

Both porous medium and variable cross-section approaches are employed in this study to propose accurate yet easy-to-use models for determining the pressure drop inside microchannels filled with arrays of micro-cylinders. To determine the accuracy and the range of applicability of both approaches, a comprehensive experimental study is carried out. For this reason, 15 samples of channels filled with arrays of micro-cylinders, covering a range of geometric parameters, are fabricated using the deep reaction ion etching (DRIE) method. Pressure drop of the samples is measured over a range of volumetric flow rates. The comparison shows that the volume averaged model predicts the experimental data over the entire range of cylinder spacing and diameter, while the results obtained from the variable cross-section method are more accurate for the samples with low cylinder spacing. Finally the utility of these models is demonstrated as we optimize the geometry of the micro-cylinder arrays to achieve the minimal flow resistance for the given surface-area-to-volume ratio. The results indicate that an optimum cylinder diameter exists for each assembly.

2. Problem formulation

The studied geometry, shown in Fig. 1, is comprised of repeating square arrangements of mono disperse cylinders, embedded in a constant cross-section rectangular microchannel. In fibrous structures, fully developed flow occurs beyond the point where the volume-averaged velocity does not change significantly along the flow. It has been stated in the literature that the fully developed condition is achieved within the first 3 rows of cylinders in the creeping flow regime; see for example [27]. Therefore, the entrance effects are neglected in the present study. As such, the flow is assumed to be steady state, incompressible and fully developed with constant fluid properties. The Knudsen number defined as the ratio of the nitrogen molecular mean free path to the smallest length scale in the tested samples is approximately 10^{-3} and we are in the border line of continuum and slip-flow flow regimes [28]. Therefore, the non-continuum effects are negligible [29,30].

2.1. Porous medium approach

In the low Reynolds number flow through porous media, the relationship between the applied pressure drop and the volume averaged (superficial) velocity is linear and can be described by the Darcy equation [31]:

$$-\frac{dP}{dx} = \frac{\mu}{K} U \quad (1)$$

where μ is the fluid viscosity and K is the permeability of the medium. For the cases where the boundary effects become significant, an additional term should be added to the right hand side of Eq. (1) to satisfy the no-slip boundary condition on solid walls, which leads to the Brinkman equation [32]:

$$-\frac{dP}{dx} = \frac{\mu}{K} U + \mu_{eff} \frac{d^2 U}{dy^2} \quad (2)$$

where μ_{eff} is the effective viscosity [31,32]. Previous studies have shown that the viscosity ratio $\mu' = \mu/\mu_{eff}$, varies between 1 to 10 [33]; therefore, various values for μ' have been employed in the literature; see [34] for more details. Tamayol et al. [21] have shown that the model of Ochoa-Tapia and Whitaker [35], which uses $\mu' = 1/\varepsilon$ is a more accurate assumption for arrays of cylinders; where ε is the porosity of the porous medium.

Tamayol et al. [21] demonstrated that for channels with small aspect ratios, i.e., $\varepsilon' = h/W < 0.1$, the problem can be envisioned

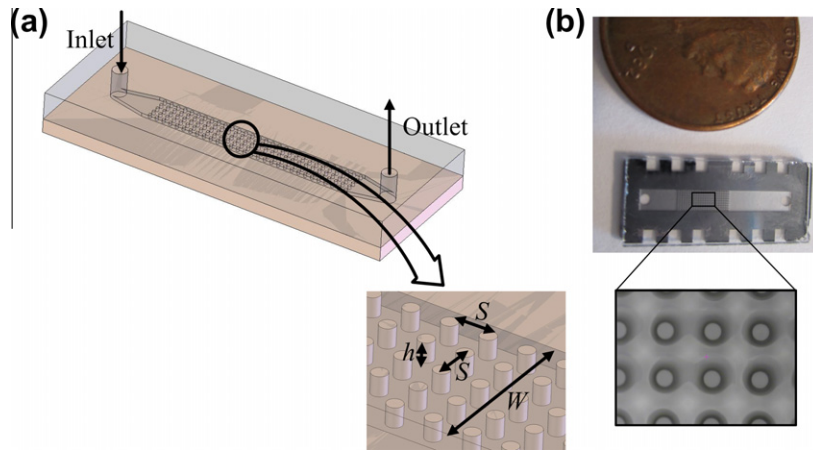


Fig. 1. Structure of the considered microchannels filled with arrays of micro-cylinders (a) the schematic, (b) a typical fabricated sample.

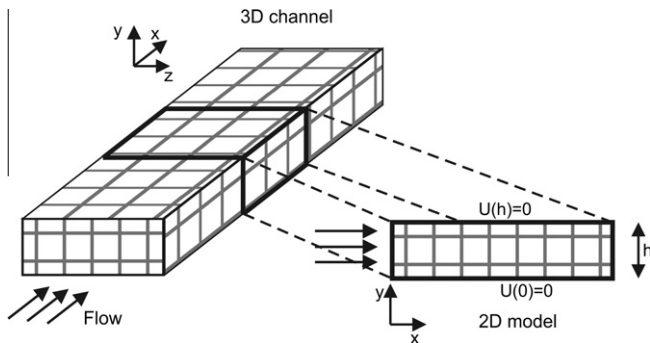


Fig. 2. Schematic of the simplified 2D model representing a porous medium sandwiched between two parallel plates.

as a porous medium sandwiched between two parallel plates, as shown in Fig. 2. Therefore, the pressure drop, ΔP , calculated from Eq. (2) becomes:

$$\frac{\Delta P}{L} = \frac{\mu Q \sinh\left(\frac{h}{\sqrt{\mu'K}}\right)}{Kh \left[2 \frac{\sqrt{\mu'K}}{h} \left[-1 + \cosh\left(\frac{h}{\sqrt{\mu'K}}\right) \right] - \sinh\left(\frac{h}{\sqrt{\mu'K}}\right) \right]}, \quad \mu' = 1/\varepsilon \quad (3)$$

To calculate the pressure drop from Eq. (3), one needs to know the permeability, K . Depending upon the microstructure of the porous medium, various relationships exist for the calculation of the permeability; see for example [11,36–38].

The permeability of infinitely long cylinders in ordered arrangements for flow normal to their axes has been studied extensively in the literature [8–12]. Recently, Tamayol and Bahrami [8] have employed an integral technique to develop an analytical model for permeability of the square arrangement of fibers. The porosity (ε) for these arrangements is determined from:

$$\varepsilon = 1 - \frac{\pi d^2}{4S^2} \quad (4)$$

where S is the distance between adjacent cylinders and d is the diameter of the cylinders, as shown in Fig. 1. The following relationship was reported for the permeability of square arrangement of fibers [8]:

$$K = \left\{ \frac{12(\sqrt{\varphi'} - 1)}{\varphi' \sqrt{\varphi'}} \left[\frac{2 - g(\varepsilon)}{2} \right] + \frac{18 + 12(\varphi' - 1)}{\sqrt{\varphi'}(1 - \varphi')^2} + \frac{18\sqrt{\varphi'} \left[\tan^{-1}\left(\frac{1}{\sqrt{\varphi' - 1}}\right) + \frac{\pi}{2} \right]^{-1}}{(\varphi' - 1)^{\frac{5}{2}}} \right\} d^2 \quad (5)$$

where $g(\varepsilon) = 1.274\varepsilon - 0.274$, and $\varphi' = \pi/4(1 - \varepsilon)$; Eq. (5) was successfully verified with experimental data collected from several sources [8]. In this study, Eq. (5) is used to calculate the permeability of the cylinders embedded inside the microchannels.

2.2. Variable cross-section approach

For low aspect ratios where the effect of walls becomes significant, following Akbari et al. [25] the investigated problem can be modeled as the fluid flow in variable cross-section microchannels of rectangular cross-section, shown in Fig. 3. They used the model of Bahrami et al. [29,39] for the pressure drop of uniform straight channels and extended it to variable cross-section channels. Using the perturbation approach, Akbari et al. [25] showed that the local Poiseuille number in slowly-varying microchannels is a weak function of the cross-sectional shape and can be obtained from the following relationship:

$$fRe_{\Gamma} = 32\pi^2 I_p^* - \frac{4\rho Q}{\mu} \left(\frac{dA/dx}{A} \right) \quad (6)$$

where ρ and μ are the fluid density and viscosity, respectively; $I_p^* = I_p/A^2$ with I_p as the polar moment of the cross-sectional area, Q is the volumetric flow rate, A is the cross-sectional area, and dA/dx indicates the rate of cross-sectional area change in the flow

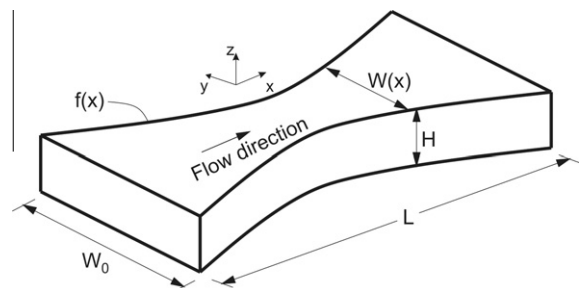


Fig. 3. Schematic diagram of a variable microchannel of rectangular cross-section with an arbitrary wall profile of $f(x)$.

direction. Using Eq. (6) for rectangular cross-section microchannels and integrating over the length of the channel, the total flow resistance can be obtained from the following relationship:

$$R = \frac{\Delta p}{Q} = 16\pi^2 \mu \int_{x_1}^{x_2} \frac{I_p^*}{A^2} dx + \rho Q \left(\frac{1}{A_2^2} - \frac{1}{A_1^2} \right) \quad (7)$$

where A_1 and A_2 are the microchannel cross-sectional area at x_1 and x_2 locations along the flow direction, respectively. I_p^* can be obtained from the following relationship:

$$I_p^*(x) = \frac{1 + \varepsilon'(x)^2}{12\varepsilon'(x)} \quad (8)$$

where $\varepsilon'(x)$ is the local cross-sectional aspect ratio of the channel such that $\varepsilon' = 1$ leads to a square cross-section. Substituting Eq. (8) into Eq. (7), under the assumption of a constant channel height one can find a closed-form solution for the pressure drop per channel length filled with circular posts of the square arrangement under the condition of $h \leq S - d$ as follows:

$$\frac{\Delta p}{L} = \frac{6\mu Q}{h^3 W} \left(\frac{\pi^2}{9} \Phi_1 + \Phi_2 \right) \quad (9)$$

where Φ_1 and Φ_2 can be calculated from the following relationships:

$$\Phi_1 = \frac{S^* (2 + 2\varphi'^2 + 3H^{*2} - 4\varphi') \left[\frac{\pi}{2} - \tan^{-1} \left(\frac{1}{\sqrt{\varphi'-1}} \right) \right]}{(\varphi' - 1)^{5/2}} + \frac{H^{*2} (5 - 2\varphi')}{\varphi' (1 - \varphi')^2} + \pi \quad (10)$$

and:

$$\Phi_2 = \frac{\sqrt{\varphi'} - 1}{\sqrt{\varphi'}} \quad (11)$$

where $H^* = h/d$. For the case of $h > S - d$, Eq. (7) should be solved numerically.

3. Experimental investigation

3.1. Microfabrication

The silicon (Si) microchannels filled with an array of micro-cylinders were created using the standard MEMS fabrication techniques to verify the trend of the proposed analytical approaches. A total of 15 samples with various diameters and spacing of micro-cylinders were designed to demonstrate the effect of porosity on the flow resistance. Each sample had the same die size, 14 by 7 mm, and the same microchannel size, 2 mm wide, 0.2 mm high, and 10 mm long. Inlet and outlet holes were placed at least 1 mm away from the posted regions to minimize the entrance and exit effects of the flow. The diameters of micro-cylinders range from 15 to 210 μm , and the micro-cylinder spacing ranges from 40 to 400 μm , covering a wide range of porosity from 0.95 to 0.33. The geometrical parameters of all the samples are summarized in Table 1.

The fabrication procedure of the microchannels with an array of micro-cylinders was reported elsewhere [14] but briefly described here. A 100-mm-diameter Si wafer (Silicon Quest International, N-type, $\langle 100 \rangle$, 1–10 Ω) was patterned with double-sided photolithography using AZ 4620 plasma-resistant photoresist (PR) and subsequently anisotropically etched in deep reactive ion etcher (Plasma-Therm SLR770). After etching about 200 μm , the PR on the wafer was stripped, and the wafer was thoroughly cleaned with the RCA clean procedure [14]. A 1-mm-thick microscope slide was cut into small pieces whose size is same as a Si die. After

Table 1

Geometrical properties of the fabricated samples; $h = 200 \mu\text{m}$ and $W = 2 \text{ mm}$.

Sample	d (μm)	S (μm)	ε	L (m)	$E(d)$ (μm)	$E(S)$ (μm)
1	54	223	0.95	0.0051	1.66	1.58
2	100	221	0.84	0.0051	0.64	2.11
3	159	218	0.58	0.0050	4.04	2.41
4	200	216	0.33	0.0050	3.01	3.64
5	203	247	0.47	0.0052	2.58	2.88
6	21	41	0.78	0.0081	1.74	1.92
7	207	253	0.48	0.0081	1.41	3.58
8	106	223	0.82	0.0080	0.63	2.09
9	208	403	0.79	0.0081	2.28	2.23
10	22	39	0.75	0.0055	0.45	1.00
11	14	40	0.90	0.0040	1.07	1.24
12	29	39	0.56	0.0039	0.85	1.37
13	19	40	0.82	0.005537	0.19	1.44
14	57	223	0.95	0.0080	1.36	1.29
15	168	222	0.55	0.0080	2.06	4.24

cleaning, a thin layer of thermally curable epoxy-based adhesive [40] was transferred to a Si die via detachment lithography [41]. A glass top was then pressed down onto the adhesive-coated Si die on a 130 °C hot plate to create a gas-tight seal. The thickness of the adhesive is less than 1 μm and applied to the substrate via the transfer printing process [41]. Therefore, the reflow of the adhesive during bonding is minimal, and the overall microchannel dimensions are unaltered even after bonding. The SEM image of an array of micro-cylinders in the microchannel is shown in Fig. 4, and the bonded Si chip is shown in Fig. 1.

3.2. Test setup

A plastic package to house the bonded sample was built using a Stereo Lithography Apparatus (SLA). Tygon® tubing and o-ring seal at the Si-package interface provided leak-free fluidic connection to a Si die. A high purity N_2 gas (S Smith, 99.9%) from the high pressure source tank was filtered and fed to the flow meter (MKS, 2179A), which regulates the flow rate of the gas via the computer software. The various flow rates used in the experiments were in the range of 0.1–35 sccm. However, the range of the tested flow rates was limited for some samples due to the maximum capacity of the employed pressure sensors. Two commercial pressure sensors (PX142, Omega Engineering Inc.) that have a linear response up to 7000 Pa with a 5 V span (giving a resolution of about 1.4 Pa mV^{-1}) are placed in the inlet and outlet of the SLA package to measure the pressure drop across the microchannel. Three independent pressure drop measurements were performed (each time

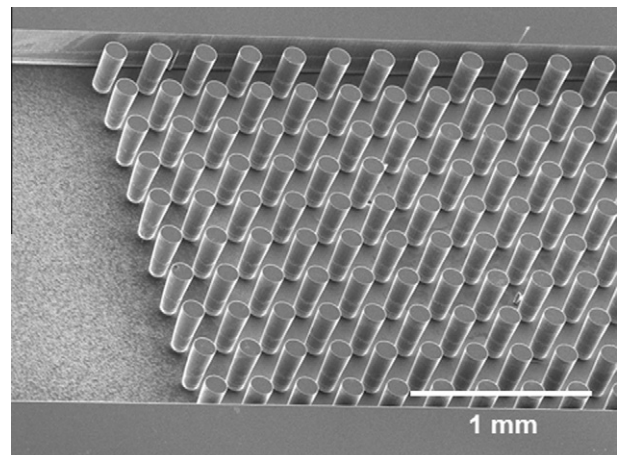


Fig. 4. A SEM image of a fabricated array of micro-cylinder arrays in silicon.

re-assembling a sample into the package) at various flow rates for each sample.

The uncertainty of the analysis is mostly a result of the uncertainty in the fabrication process and the uncertainty in the channel and cylinder size measurements. A calibrated optical microscope was used to record the channel and micro-cylinder dimensions. Five independent measurements were obtained for each sample and the average values were used in the analysis. The maximum uncertainties, associated with the measured values for micro-cylinder diameters and the distance between adjacent posts, are listed in Table 1. In addition, the uncertainty of the measured values of flow resistance in various trials and flow rates for each sample, included in the plots, was calculated as follows [42]:

$$\frac{E(\Delta P/Q)}{(\Delta P/Q)} = \sqrt{\left(\frac{E(\Delta P)}{\Delta P}\right)^2 + \left(\frac{E(Q)}{Q}\right)^2} \quad (12)$$

where $E(\cdot)$ indicated the uncertainty associated with the involved parameters. The uncertainty in the measured values was less than 10%.

4. Results and discussion

The values of flow resistance ($\Delta P/Q$) obtained by the porous medium approach, Eqs. (3) and (5), and the variable cross-section method, Eq. (7), are compared with the experimental data in Figs. 5 and 6 for some of the tested samples. Consistent with the creeping flow assumption, it can be seen that the experimental values of $\Delta P/Q$ remain constant over the investigated range of flow rates.

The accuracy of the porous medium and the variable cross-section approaches is investigated in Figs. 7 and 8 where the experimental data are plotted versus the predicted flow resistance for all the samples. It can be observed that both methods can predict the trend of the experimental data. However, the porous medium approach is more flexible and shows good agreement over the entire range of porosity; the maximum deviation between the model and the experimental data is less than 25%, which is reasonable within the context of porous media and microfluidics. It should be noted that this approach is also applicable to analyzing flow through channels filled with other types of fibrous porous media;

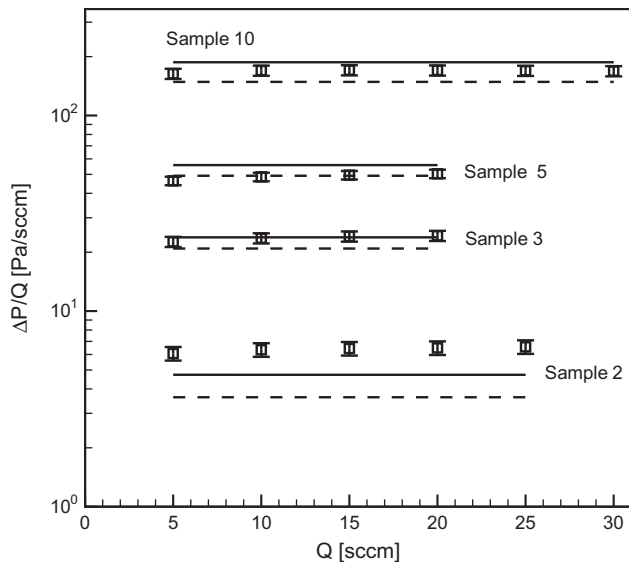


Fig. 5. Flow resistance versus flow rate for samples 2, 3, 5, and 10. Hollow symbols show the experimental data; solid lines present the values predicted by porous medium (Eqs. (3) and (5)) and dashed lines present variable cross-section approaches (Eq. (7)).

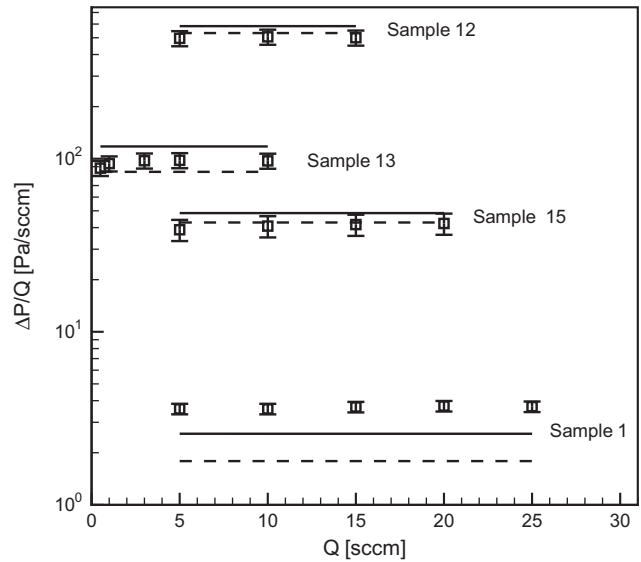


Fig. 6. Flow resistance versus flow rate for samples 1, 12, 13, and 15. Symbols show the experimental data; solid lines present the values predicted by porous medium (Eqs. (3) and (5)) and dashed lines present variable cross-section approaches (Eq. (7)).

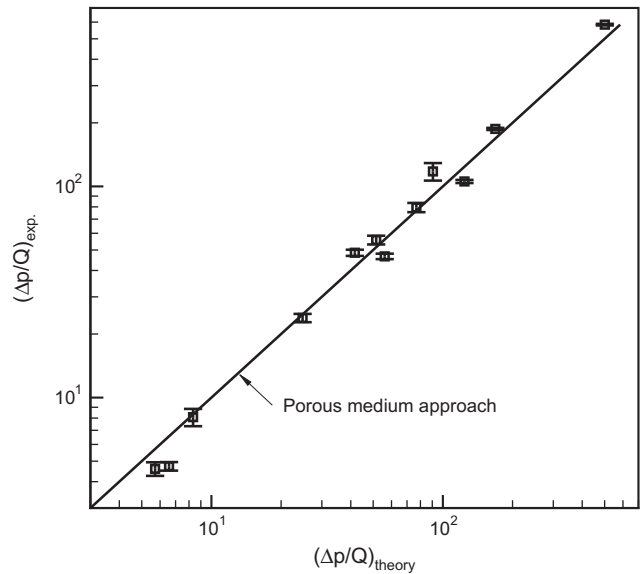


Fig. 7. Experimental values of flow resistance versus the values predicted by porous medium approach, Eqs. (3) and (5).

however, the permeability should be known beforehand. It should be noted that in general, there is a competing trend between the channel height and the permeability of the micro-cylinder array on dominating the pressure drop of the samples. Increasing the aspect ratio reduces the importance of the channel walls on the pressure drop. For more details please refer to [21].

The variable cross-section technique on the other hand is more accurate for geometries where the ratio of the gap spacing to the cylinder size and channel height is small. But as the porosity of the structure and the gap sizes increases, the deviation from channel flow becomes more pronounced and variable cross-section model is less accurate; see for example in samples 1 and 2.

Now that the proposed models have been verified experimentally they can be used for investigating the effect of various parameters such as micro-cylinder diameter on the surface-to-volume

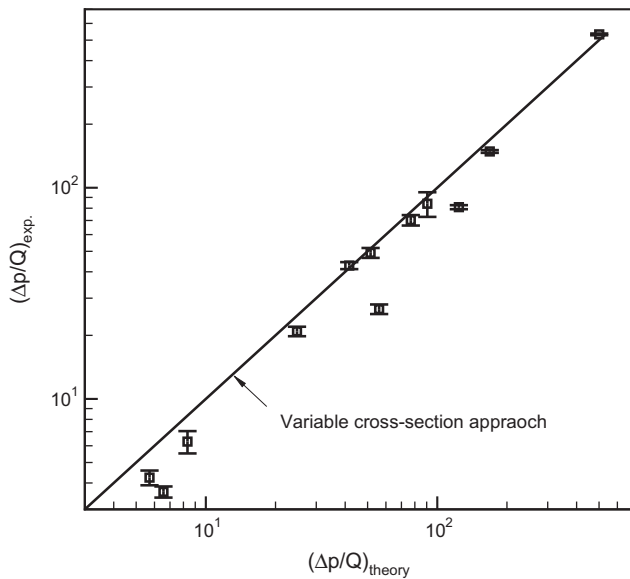


Fig. 8. Experimental values of flow resistance versus the values predicted by variable cross-section approach, Eq. (7).

ratio and pressure drop of microchannels filled with micro-cylinders. To perform a parametric study, a typical microchannel with the width of 2000 μm and the height of 200 μm is considered. A range of cylinder diameters from 2 μm to 100 μm is considered. The spacing between micro-cylinders embedded in the channel is controlled by changing the number of cylinders from 2 to 500. It should be noted that in general, adding micro-cylinders enhances surface-area-to-volume ratio at the expense of an increase in the overall pressure drop. The surface-area-to-volume ratio and the pressure drop for each design is calculated from the geometrical relationship and Eqs. (3) and (5), respectively.

Fig. 9 shows the flow resistance as a function of the surface-area-to-volume ratio. It can be seen that the micro-cylinder diameter has a significant impact on both the surface-area-to-volume ratio and the pressure drop; however, the relationship is non-linear. In general, one can say that using smaller cylinders

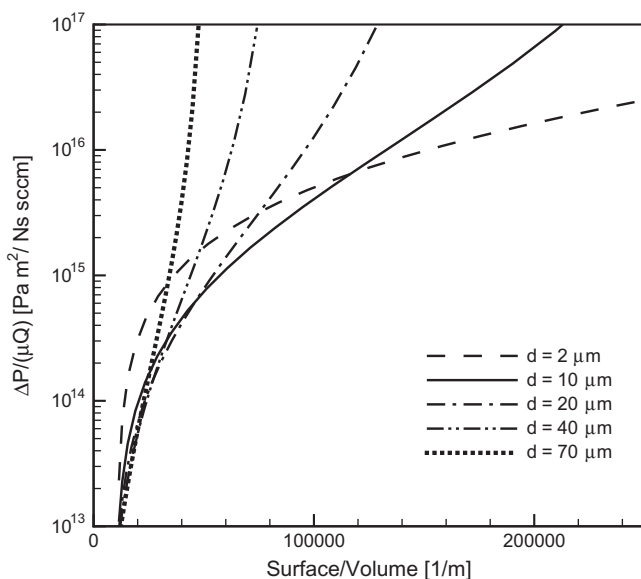


Fig. 9. Flow resistance versus effective surface area for various micro-cylinder diameters; $L = 0.01$ m, $W = 2000$ μm , and $h = 200$ μm .

(2 μm in diameter) can result in structures with high surface-area-to-volume ratio with a lower pressure drop. However, if a small surface area is required, structures formed by micro-cylinders with larger diameters have lower pressure drops.

The optimum diameter of the micro-cylinders depends on the desired surface-area-to-volume ratio and the channel geometry. Thus, we could not find a compact correlation for the optimum cylinder diameter. However, the use of micro-cylinders with few micrometers in diameters and nanostructures can reduce the overall pressure drop of a fabricated sample while maintaining the surface-area-to-volume ratio.

5. Summary and conclusions

Two independent modeling approaches, i.e., porous medium and flow in variable cross-section microchannels, were used to determine the pressure drop of ordered arrays of cylinders embedded inside microchannels. Compact relationships were proposed for predicting the flow resistance as a function of the involved geometrical parameters such as micro-cylinder diameter, spacing between adjacent cylinders, channel height, and width. To verify the developed models, 15 silicon/glass samples were fabricated using the deep reacting ion etching (DRIE) technique. Pressure drop measurements were performed over a wide range of nitrogen flow rates spanning from 0.1 sccm to 35 sccm. It was observed that both methods captured the trend of the experimental data. The variable cross-section technique was more accurate for dense arrays of micro-cylinders and for highly porous structures the deviations from the experimental data became more pronounced. The porous medium approach on the other hand showed a wider range of applicability with reasonable accuracy. Our results suggest that an optimal micro-cylinder diameter exists that minimizes the pressure drop for the specific surface-area-to-volume ratio. This diameter is a function of the channel dimensions and the desired surface-area-to-volume ratio. The proposed models and the related analysis can provide a powerful tool for designing energy efficient micro-reactors in which an array of micro-cylinders provides high surface areas for enhanced heat and mass transfer without causing undue pressure drops.

Acknowledgments

Financial support of the Natural Science and Engineering Research Council (NSERC) of Canada is gratefully acknowledged. A.T. and M.A. thank British Columbia Innovation Council (BCIC) for financial support through Innovation Scholar awards. Authors would like to thank Professor Mark A. Shannon for useful discussions and generously allowing the authors to use his research facilities.

References

- [1] M. Roumanie, C. Pijolat, V. Meille, C. De Bellefon, P. Pouteau, C. Delattre, Deposition of Pt-catalyst in a micro-channel of a silicon reactor: application to gas micro-TAS working at high temperature, *Sensor Actuat. B: Chem.* 118 (1–2) (2006) 297–304.
- [2] M.W. Losey, R.J. Jackman, S.L. Firebaugh, M.A. Schmidt, K.F. Jensen, Design and fabrication of microfluidic devices for multiphase mixing and reaction, *J. Microelectromech. Syst.* 11 (6) (2002) 709–717.
- [3] A. Kosar, C. Mishra, Y. Peles, Laminar flow across a bank of low aspect ratio micro pin fins, *J. Fluids Eng.* 127 (3) (2005) 419–430.
- [4] Y. Peles, A. Kosar, C. Mishra, C.J. Kuo, B. Schneider, Forced convective heat transfer across a pin fin micro heat sink, *Int. J. Heat Mass Transfer* 48 (17) (2005) 3615–3627.
- [5] N.S.K. Gunda, J. Joseph, A. Tamayol, M. Akbari, S.K. Mitra, Measurement of pressure drop and flow resistance in microchannels with integrated micropillars, *Microfluid. Nanofluid.*, in press, <http://dx.doi.org/10.1007/s10404-012-1089-1>.
- [6] S. Nagrath, L.V. Sequist, S. Maheswaran, D.W. Bell, D. Irimia, L. Ulkus, M.R. Smith, E.L. Kwak, S. Digumarthy, A. Muzikansky, P. Ryan, U.J. Balis, R.G. Tompkins, D.A. Haber, M. Toner, Isolation of rare circulating tumour cells in

- cancer patients by microchip technology, *Nature* 450 (7173) (2007) 1235–1239.
- [7] Y. Yong-Kyu, P. Jung-Hwan, F. Cros, M.G. Allen, Integrated vertical screen microfilter system using inclined SU-8 structures, in: *Micro Electro Mechanical Systems, MEMS-03 Kyoto, IEEE The 16th Annual International Conference on 2003, 2003*, pp. 227–230.
- [8] A. Tamayol, M. Bahrami, Analytical determination of viscous permeability of fibrous porous media, *Int. J. Heat Mass Transfer* 52 (9–10) (2009) 2407–2414.
- [9] M. Sahraoui, M. Kaviany, Slip and no-slip velocity boundary conditions at interface of porous, plain media, *Int. J. Heat Mass Transfer* 35 (4) (1992) 927–943.
- [10] J. Happel, Viscous flow relative to arrays of cylinders, *AIChE J.* 5 (2) (1959) 174–177.
- [11] A. Tamayol, M. Bahrami, Transverse permeability of fibrous porous media, *Phys. Rev. E* (2010).
- [12] J.P.D. Plessis, Analytical quantification of coefficients in the Ergun equation for fluid friction in a packed bed, *Transp. Porous Med.* 16 (2) (1994) 189–207.
- [13] S. Vanapalli, H.J.M.t. Brake, H.V. Jansen, J.F. Burger, H.J. Holland, T.T. Veenstra, M.C. Elwenspoek, Pressure drop of laminar gas flows in a microchannel containing various pillar matrices, *J. Micromech. Microeng.* 17 (7) (2007) 1381.
- [14] J. Yeom, D.D. Agonafer, J.H. Han, M.A. Shannon, Low Reynolds number flow across an array of cylindrical microposts in a microchannel and figure-of-merit analysis of micropost-filled microreactors, *J. Micromech. Microeng.* 19 (6) (2009) 065025.
- [15] A. Haji-Sheikh, Fully developed heat transfer to fluid flow in rectangular passages filled with porous materials, *J. Heat Transfer* 128 (6) (2006) 550–556.
- [16] A. Haji-Sheikh, W.J. Minkowycz, E.M. Sparrow, Green's function solution of temperature field for flow in porous passages, *Int. J. Heat Mass Transfer* 47 (22) (2004) 4685–4695.
- [17] A.V. Kuznetsov, M. Xiong, D.A. Nield, Thermally developing forced convection in a porous medium: circular duct with walls at constant temperature, with longitudinal conduction and viscous dissipation effects, *Transp. Porous Med.* 53 (3) (2003) 331–345.
- [18] K. Hooman, H. Gurgenci, Porous medium modeling of air-cooled condensers, *Transp. Porous Med.* 84 (2) (2010) 257–273.
- [19] G.R. Imani, M. Maerefat, K. Hooman, Estimation of heat flux bifurcation at the heated boundary of a porous medium using a pore-scale numerical simulation, *Int. J. Therm. Sci.* 54 (2012) 109–118.
- [20] G. Gamrat, M. Favre-Marinet, S. Le Person, R. Baviere, F. Ayela, An experimental study and modelling of roughness effects on laminar flow in microchannels, *J. Fluid Mech.* 594 (2008) 399–423.
- [21] A. Tamayol, A. Khosla, B.L. Gray, M. Bahrami, Creeping flow through ordered arrays of micro-cylinders embedded in a rectangular minichannel, *Int. J. Heat Mass Transfer* 55 (15–16) (2012) 3900–3908.
- [22] D. Erickson, D. Sinton, D. Li, Joule heating and heat transfer in poly (dimethylsiloxane) microfluidic systems, *Lab Chip* 3 (2003) 141–149.
- [23] M. Akbari, D. Sinton, M. Bahrami, Pressure drop in rectangular microchannels as compared with theory based on arbitrary cross section, *J. Fluids Eng.* 131 (4) (2009). 041202–041201–041208.
- [24] M. Akbari, D. Sinton, M. Bahrami, Laminar fully developed flow in periodically converging–diverging microtubes, *Heat Transfer Eng.* 31 (8) (2010) 628–634.
- [25] M. Akbari, D. Sinton, M. Bahrami, Viscous flow in variable cross-section microchannels of arbitrary shapes, *Int. J. Heat Mass Transfer* (2011).
- [26] R. Wild, T.J. Pedley, D.S. Riley, Viscous flow in collapsible tubes of slowly varying elliptical cross-section, *J. Fluid Mech.* 81 (2) (1977) 273–294.
- [27] W. Zhong, I. Currie, D. James, Creeping flow through a model fibrous porous medium, *Exp. Fluids* 40 (1) (2006) 119–126.
- [28] A. Tamayol, K. Hooman, Slip-flow in microchannels of non-circular cross sections, *J. Fluids Eng.* 133 (9) (2011) 091202.
- [29] M. Bahrami, A. Tamayol, P. Taheri, Slip-flow pressure drop in microchannels of general cross section, *J. Fluids Eng.* 131 (3) (2009) 031201.
- [30] M. Renssizbulut, H. Niazmand, G. Tercan, Slip-flow and heat transfer in rectangular microchannels with constant wall temperature, *Int. J. Therm. Sci.* 45 (9) (2006) 870–881.
- [31] M. Kaviany, *Principles of Heat Transfer in Porous Media*, second ed., Springer-Verlag, New York, 1995.
- [32] H.C. Brinkman, A calculation of the viscous force exerted by a flowing fluid on a dense swarm of particles, *Appl. Sci. Res.* 1 (1) (1949) 27–34.
- [33] R.C. Givler, S.A. Altobelli, A determination of the effective viscosity for the Brinkman–Forchheimer flow model, *J. Fluid Mech.* 258 (1) (1994) 355–370.
- [34] A. Tamayol, K. Hooman, M. Bahrami, Thermal analysis of flow in a porous medium over a permeable stretching wall, *Transp. Porous Med.* 85 (3) (2010) 661–676.
- [35] J.A. Ochoa-Tapia, S. Whitaker, Momentum transfer at the boundary between a porous medium and a homogeneous fluid–I. Theoretical development, *Int. J. Heat Mass Transfer* 38 (14) (1995) 2635–2646.
- [36] A. Tamayol, F. McGregor, M. Bahrami, Single phase through-plane permeability of carbon paper gas diffusion layers, *J. Power Sour.* 204 (2012) 94–99.
- [37] B.T. Astrom, R.B. Pipes, S.G. Advani, On flow through aligned fiber beds and its application to composites processing, *J. Compos. Mater.* 26 (9) (1992) 1351–1373.
- [38] M.M. Tomadakis, T.J. Robertson, Viscous permeability of random fiber structures: comparison of electrical and diffusional estimates with experimental and analytical results, *J. Compos. Mater.* 39 (2) (2005) 163–188.
- [39] M. Bahrami, M.M. Yovanovich, J.R. Culham, A novel solution for pressure drop in singly connected microchannels of arbitrary cross-section, *Int. J. Heat Mass Transfer* 50 (13–14) (2007) 2492–2502.
- [40] B.R. Flachsbarth, K. Wong, J.M. Iannacone, E.N. Abante, R.L. Vlach, P.A. Rauchfuss, P.W. Bohn, J.V. Sweedler, M.A. Shannon, Design and fabrication of a multilayered polymer microfluidic chip with nanofluidic interconnects via adhesive contact printing, *Lab Chip* 6 (5) (2006) 667–674.
- [41] J. Yeom, M.A. Shannon, Detachment lithography of photosensitive polymers: a route to fabricating three-dimensional structures, *Adv. Funct. Mater.* 20 (2) (2010) 289–295.
- [42] J.R. Taylor, *An introduction to error analysis: the study of uncertainties in physical measurements*, second ed., University Science Books, Sausalito, USA, 1997.